Nanomed. J. 6(2): 85-96, Spring 2019

RESEARCH PAPER

Entrapped chemically synthesized gold nanoparticles combined with polyethylene glycol and chloroquine diphosphate as an improved antimalarial drug

Shittu Oluwatosin Kudirat [1*], Abdulrasheed Tawakalitu [2], Abdulkareem A. Saka [3], Abubakre O. Kamaldeen [4], Bankole Mercy T [2], Tijani, Jimoh Oladejo [2]

[1] Biochemistry Department, Federal University of Technology, Bosso, Nigeria
[2] Chemical Engineering Department, Federal University of Technology, Minna, Nigeria
[3] Mechanical Engineering Department, Federal University of Technology, Minna, Nigeria
[4] Chemistry Department, Federal University of Technology Minna, Nigeria

ABSTRACT

Objective(s): Drug delivery is an engineering technology to control the release and delivery of therapeutic agents to target organs, tissues, and cells. Metallic nanoparticles, such as gold nanoparticles (AuNPs) have exceptional properties which enable efficient drug transport into different cell types with reduced side effects and cytotoxicity to other tissues.

Materials and Methods: AuNPs were synthesized by adopting the Turkevich method to reduce tetra chloroauric (III) acid (HAuCl4) solution with sodium citrate. A factorial design of 24 was used to investigate the influence of temperature, stirring speed, and the volume of citrate and gold salt on the size of AuNPs synthesis. The produced chemical-AuNPs (CN-AuNPs) were characterized using ultraviolet-visible spectroscopy and dynamic light scattering (DLS) which was conjugated with polyethylene glycol (PEG) loaded with chloroquine diphosphate. The latter were characterized with transmission electron microscopy (TEM), Energy dispersive x-ray spectroscopy (EDS), selected area electron diffraction (SAED) patterns and Fourier transmission infrared spectroscopy. The antimalarial activities of the three formulations were tested on Plasmodium-infected mice. Moreover, the evaluation of curative potentials of the formulations was carried out via parasite counts. The anemic and pathological conditions of nano-encapsulation were investigated for their cytotoxicity level.

Results: The CN-AuNPs show surface plasmon resonance absorption ranging from 526 to 529 nm with smaller particle size at the lower citrate volume. The TEM image of CN-AuNPs with polyethylene glycol (PEG) and CN-AuNPs-PEG encapsulated with chloroquine diphosphate revealed spherical shape with EDS showing the appearance of gold (Au) at 2.0, 2.1, and 9.9 KeV. The SAED also revealed that the AuNPs were crystalline in nature. The in vitro time-dependent encapsulation release showed an extension of time release, compared to CN-AuNPs-PEG with parasitemia clearance at the same level of cytotoxicity.

Conclusion: Therefore, although improved activity of the CN-AuNPs-PEG encapsulating was achieved but its cytotoxicity still is a limitation.

Keywords: *Chemical synthesis, Characterization, Chloroquine diphosphate, Encapsulation, Gold nanoparticles*

How to cite this article

Oluwatosin Kudirat Sh, Tawakalitu A, A. Saka A, O. Kamaldeen A, Mercy T B, Jimoh Oladejo T. Entrapped chemically synthesized gold nanoparticles combined with polyethylene glycol and Chloroquine diphosphate as an improved antimalarial drug. Nanomed J. 2019; 6(2): 85-96. DOI: 10.22038/nmj.2019.06.0002

INTRODUCTION

Malaria is a global disease that is predominant in the tropics and has greater morbidity and mortality rates than any other infectious diseases throughout the world (World Malarial Report, 2005; World Health Organization, 2000). Survey has shown that 90% of the world's cases of malaria occur in sub-Saharan Africa with nine out of ten cases occur in this region leading to over one million deaths annually (World Malarial Report, 2005; Africa Union Memoir, 2005). The parasites that cause this disease have been reported to exhibit resistance to available chemotherapies. These chemotherapies are divided into groups and the first one is quinoline-based antimalarial,

* *Corresponding Author Email: toscueyusuf@futminna.edu.ng*
Note. This manuscript was submitted on October 30, 2018; approved on February 15, 2019

which includes quinine and its derivatives, such as Chloroquine (CQ), Amodiaquine, Primaquine, and Mefloquine.

Chloroquine is also known as Chloroquine phosphate ($C_{18}H_{26}ClN_3.2H_3PO_4$) and was discovered in the 1940s. It is regarded as a synthetic 4-aminoquinoline with less toxic and well tolerable effective antimalarial which is structurally similar to quinine.

This drug was cheap, non-toxic, and effective against all strains of the parasite; therefore, it became the mainstay of prevention. The resistance was developed by Plasmodium falciparum which rendered it useless in most endemic areas as the first line of treatment [2].

In view of this, the eradication of this disease requires technology fronts that can address the limitation of this chemotherapy [3]. Nanotechnology is a dynamic field of science and engineering that produces materials with dimensions up to 100 nanometer in size. Moreover, it has potential applications in improving the efficacy of current chemotherapies. These potentials are attributed to nanoparticle scale and dimension which include higher stability when they are in contact with biological fluids. In addition, their high drug-loading capacities, and the protection of the solid matrix of the incorporated drug against degradation lead to an increased intracellular concentration of the drug [4].

Other properties of nanoparticles include a high surface area to volume ratio and excellent optical, physical, electrical, and mechanical properties [5]. Of all the nanoparticles, metallic nanoparticles are of peaked interests owing to their intrinsic tunable optical properties that are of importance for the treatment and diagnosis of the diseases [6].

The ease of tailoring gold nanoparticles into different size, shape, and decorations with different functionalities encourages the researchers to explore the ultimate potentials of gold nanoparticles for biomedicine purposes, especially for drug delivery and imaging [7]. Based on the identified potential of gold nanoparticles, they have emerged as a promising delivery system for efficient transport and release of pharmaceuticals into diverse cell types as a covalent or non-covalent conjugate to incorporate multiple therapeutic drugs or biomacromolecules [8]. The potential applications of AuNPs have been studied and administrated in phases I and II clinical trials for cancer treatment [9].

The conventional method of gold nanoparticle synthesis includes chemical, biological, and physical methods, such as chemical reduction, pyrolysis, and laser ablation. Kumar et al. [10] reported that the synthesis of the gold nanoparticle using sodium citrate as a reducing agent was successful and Au/citrate ratio has a significant effect on nanoparticle size. Active pharmaceutical ingredient is a term used to refer to an active component of the drug. It is almost never administered alone and usually formulated with other component called excipients. These excipients are reported to be added to formulations in order to improve the bioavailability of the drug and the acceptance by the patients [11, 12].

Polyethylene glycol is a hydrophilic, non-ionic polymer which exhibits exceptional biocompatibility. The most preferred process of surface modification is the adsorption of PEG to the surface of the nanoparticle [13]. The addition of PEG to the surface of particles results in an augment in the blood circulation half-life of the nanoparticles, thereby increasing the residency of the nanoparticles in the blood [14]. In recent years, nanoparticles have been used for developing formulations with special features, and the research on the nanoparticle-based drug delivery systems has dominated the literature [15]. Significant advances have been made on drug delivery and Joshi et al. investigated the binding of Chloroquine conjugated gold nanoparticles with bovine serum albumin (BSA) [16].

In this case, the author reported that GNP-Chloroquine interacted efficiently with BSA and the thermodynamic parameters suggested that the binding was driven by both enthalpy and entropy. Therefore, unraveling the nature of interactions of GNP-Chl with BSA paved the way for the design of nanotherapeutic agents with improved functionality.

Don Zhang et al. [17] conducted a study on size-dependent in vivo toxicity of PEG-coated gold nanoparticles synthesized chemically. The results showed no adverse effects of AuNPs on the growth of treated mice with the synthesized gold nanoparticles for 28 days. In addition, Movellan et al. [18] utilized amphiphilic derivatives as nanocarriers for targeted delivery of antimalarial drugs as dendrimers and dendrons.

These polymers have the possibility of precisely

tailoring their structure and are considered excellent candidates to design nano aggregates that can be used as vehicles for drug delivery. The studies revealed that free Chloroquine reduces parasitemia better than conjugation; however, the survival rates were better in mice treated with conjugated Chloroquine, compared to those treated with free Chloroquine.

In the same vein, Urban et al. [19] employed Chloroquine and conjugated primaquine to either AGMAI or ISA23 (a polyamide amine derivatives) for antimalarial drug delivery to Plasmodium-infected red blood cells. According to the results, the AGMA1- and ISA23-Chloroquine polymeric salts were remarkably more effective in vivo than the free drug which makes them have potential as an antimalarial. However, the nanoparticle-based formulations drastically improved the goals of developing unique delivery systems.

The aim of this study was to investigate the optimum condition for chemically synthesized gold nanoparticle and bioavailability of the formulated encapsulation for antiplasmodial activities.

MATERIALS AND METHODS

All the chemicals used are of analytical grades with percentage purity in a range between 99 and 99.9%. Hydrogen tetra auric acid ($HAuCl_4$) and polyethylene glycol was the product of Sigma Aldrich Company, USA.

Experimental animals and parasite

Healthy albino mice with average weight of 25-30 g and Plasmodium berghei NK65 (Chloroquine-sensitive strain) were obtained from Animal Holding Unit, Department of Pharmacy Ahmadu Bello University, Zaria, Nigeria. The rodents were kept in clean plastic cages and maintained under standard laboratory conditions.

Table 1. Variation parameters based on particle size using factorial design for the gold nanoparticles

Variables	pH of reaction mixture	Stirring speed (rpm)	Stirring time (min)
Low level (-)	2	120	1
High level (+)	10	250	20

METHODS

Synthesis of gold nanoparticles

Design expert software was used to design a 2^4 factorial experiment using the process variable levels shown in table 1. An experiment containing 16 runs was designed using the software for each variable condition, such as temperature, stirring speed, and the volumes of citrate and gold salt. After the synthesis of gold nanoparticles, aqua regia solution was used for the cleaning of the apparatus followed by rinsing with deionized water and proper draining.

A stock solution of (1mM) $HAuCl_4$ and (1wt %) sodium citrate was prepared in deionized water and stored at room temperature. Thereafter, 10 ml of stock solution was heated on a magnetic hot plate at stirring speeds of 450 and 500 (rpm) and temperature of 80°C and 100°C until it boiled.

This was followed by the rapid addition of 1 mL of 1% of trisodium citrate (as reducing agents) through the condenser. A dark red coloration was produced which indicated the reduction of Au^{3+} to Au^0.

The heating process was stopped and the sand bath was removed while stirring continued to allow cooling of the sample to room temperature. These procedures were then repeated for other runs.

The reaction mechanisms of gold nanoparticles are presented in equations 1 and 2.

$Na_3C_6H_8O_7$ + Deionised water $Na_3C_6H_8O_7$ solution.(1)

$HAuCl_4$ (yellow color) + $Na_3C_6H_8O_7Au^0$ (dark red color) (2)

Encapsulation of the composite

The encapsulation process was carried out using Chloroquine phosphate (standard drug) and polyethylene glycol (Molecular Weight = 2000). Three formulations of the composites were made.

The first encapsulation comprised of the Chloroquine phosphate coated with AuNPs and PEG. It was prepared by the addition of 0.5 mL of gold nanoparticles (AuNPs) with 2 g of PEG and 0.5 g of the Chloroquine phosphate under constant stirring speed for one hour.

The second formulation comprised of 0.5 mL of AuNPs with 2 g PEG and was stirred for one hour. The third formulation was prepared by mixing 0.5g of the Chloroquine diphosphate with 1 mL sterile deionized water.

This was followed by the addition of 2g of PEG and stirring period of one hour [20].

All the formulations were made into tablet form by incubating at 37°C for two h to enable digestion and properly air dried hereafter.

The first formulation: PCNCQ=PEG+CN+CQ
The second formulation: PCN=PEG+CN
The third formulation: PCQ=PEG+CQ

Characterization of chemically synthesized gold nanoparticles and encapsulations

The ultraviolet-visible spectroscopy (UV-vis), which is the most commonly used technique for characterization of noble nanoparticles, was employed to measure the optical of the sample produced in the range of 200-800 nm using a UV-1800 Shimadzu spectrophotometer.

The particle size and the distribution of the gold nanoparticles were measured with dynamic light scattering equipment Malvern zetasizer nano (Nano-S model).

The morphological shape of the three encapsulates was carried out using a transmission electron microscopy (TEM) performed on a JEOL model 1200EX instrument at the University of Western Cape, South Africa. The elemental composition of the encapsulation was analyzed using energy-dispersive x-ray spectroscopy (EDS) S-3400N and the selected area electron diffraction (SAED) pattern was done.

In vitro encapsulated release studies

The in vitro encapsulated release studies were carried out for PCND and PD containing 0.5 mL of (AuNPs), 2 g of PEG, and free Chloroquine phosphate 5 mg/ml in 3 ml of phosphate buffer solution at room temperature. Serial withdrawals from PCND and PD solutions were carried out at intervals of 3 min.

The absorbance relationship with the concentration of each solution was evaluated using UV-vis spectrophotometer, compared to 5 mg/ml concentration of free Chloroquine phosphate at zero minutes.

Inoculation of experimental animal and parasitized cell count

Parasitized erythrocytes were obtained from the jugular vein of Plasmodium berghei donor-infected mouse into an EDTA- bottle and diluted appropriately with phosphate buffer saline (PBS). The diluted blood suspension of 0.2 ml was used to inoculate healthy mice intraperitoneally and allowed 72 hr lag phase growth before microscopic examination of blood smears. The blood smear slides were allowed to dry and fixed with methanol and stained with Giemsa solution for 30 min before the parasitized cell count was done by microscopic examination of Wright's-stained thin-blood smears [18].

Cytotoxicity studies

The histopathological evaluation of the liver and kidney of the experimental group treated with PCND, PD, and free Chloroquine diphosphate as well as the control group were carried out at the University of Ilorin Teaching Hospital, Nigeria. Various organs were placed in an embedded cassette and thereafter fixed with 10% formalin for 1 hr and subsequently dehydrated with methanol (70, 90 and 100%) at different concentrations and times.

The 2 hr clearing with xylene was done using alcohol and xylene, which prepared the tissue for waxing. Moreover, the mounting medium, dibutyl phthalate xylene, was dropped on the tissue section and then viewed under the microscope.

Ethical considerations

The principles governing the use of laboratory animals as laid out by the Federal University of Technology, Minna, Nigeria, were adopted based on Committee on Ethics for Medical and Scientific Research. Moreover, this was based on the Canadian Council on Animal Care Guidelines and Protocol contained the existing internationally accepted principles for laboratory animal use and cares.

Statistical analysis

The data were analyzed in SPSS software (version 16). The ANOVA was used to compare the differences between groups followed by Duncan's Multiple Range Test.

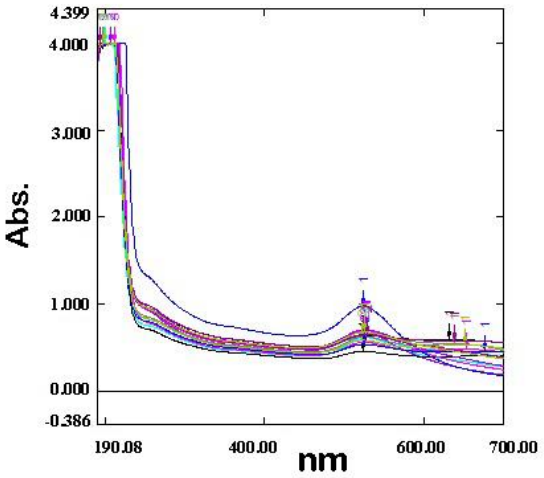

Fig 1. UV-Visible spectra of synthesized AuNPs

RESULTS

Ultraviolet-Visible spectroscopy

Fig 1 shows the UV-vis spectra of CN-AuNPs synthesized with four different process variables based on factorial experimental design. The peaks between 524 and 529 nm correspond to surface Plasmon resonance effect which is the characteristic of AuNPs. The movement of these shifts from 180 nm to higher wavelengths of 524 and 529 nm indicates changes in particle diameter to nano size, whereas the absorbance provides information on AuNP concentration.

Based on the variable conditions, it was observed that an increase in temperature from 80°c to 100°c shift the spectra to a lower wavelength. This suggests a decrease in particle size which can be due to the availability of enough kinetic energy to effect molecular movement of the nanoparticles leading to the prevention of particle aggregation.

In a study conducted by Kumar et al. [21] on controlling the size and size distribution of gold nanoparticles, it was revealed that higher synthesis temperature led to a blue shift suggesting a decrease in particle size.

Other factors affecting the position of the peak in the UV-vis spectra significantly include volume ratio of gold salt to citrates (reducing agents), a decrease in volume of citrate used for the reduction leading to the broadening of the UV-vis peak, and a shift to higher frequencies. This indicates an increase in particle size and a widening of the size distribution. Moreover, an increase in volume from 1 to 2 ml by reducing agents shifts the spectra to lower wavelength. The observed trend of the shift may be due to the availability of enough reducing agents which increases the rate of nucleation of particles leading to a smaller average particle sizes.

Kumar et al., [22] reported that high levels of citrate equivalent to a low Au/citrate ratio resulted in the narrowing of the UV-vis peak and a shift to lower frequencies. In addition, increased stirring rate led to a downshift in the UV-vis peak which was indicative of a reduction in nanoparticle size.

A higher UV-vis absorbance was also noted with increased stirring rate indicating a higher concentration of AuNPs and a more complete reaction. Young et al. [23] conducted a study on the effect of stirring on the size and distribution using CO gas. The results showed that more monodispersed nanoparticles were observed at higher stirring rates.

The UV-vis data revealed that temperature and stirring rate did not have significant effects on particle size.

Dynamic light scattering from gold nanoparticles for particle size

The average particle size obtained from each sample under different process conditions is shown in Fig 2. Based on the variable conditions, it can be observed that the reduction of the amount of citrate during synthesis increases particle diameter. Moreover, bimodal size distributions of a significant proportion of very large particles result from the use of lower citrate volume. Wolfgang et al. [24] reported that both very

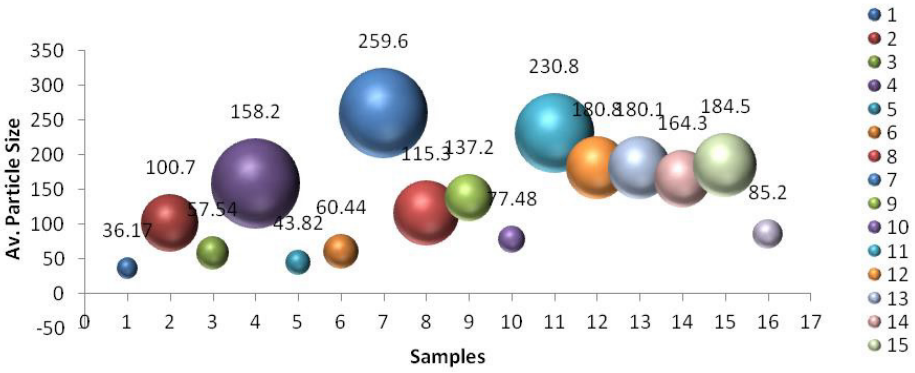

Fig 2. Average particle sizes of AuNPs synthesized with variable conditions

Table 2. UV-visible spectra of chemically synthesized gold nanoparticles

Sample No	Temp. (^{0}C)	Stirring Speed(rpm)	Vol.of Citrate(ml)	Vol.of $H(AuCl_4)$(ml)	UV-VIS Wavelength
1	100	500	2	15	526
2	80	450	2	15	526
3	100	450	2	15	529
4	100	450	1	15	529
5	100	500	2	10	524
6	80	500	1	10	526
7	80	500	1	15	528
8	80	450	1	10	524
9	100	450	2	10	524
10	80	450	2	10	527
11	100	450	1	10	523
12	100	500	1	15	525
13	80	450	1	15	528
14	100	500	1	10	526
15	80	500	2	15	529
16	80	500	2	10	527

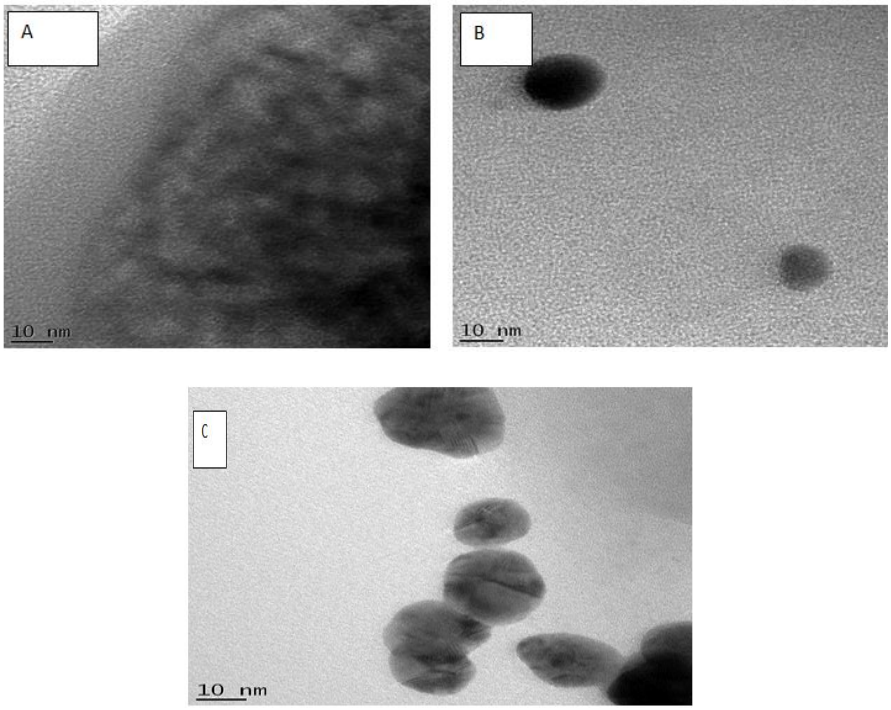

Fig 3. (A) The TEM of polyethylene glycol and Chloroquine diphosphate; (B) TEM of chemicalsynthesized gold nanoparticles encapsulated with polyethylene glycol and Chloroquinediphosphate (C) TEM of chemical synthesized gold nanoparticles encapsulate with polyethylene glycol

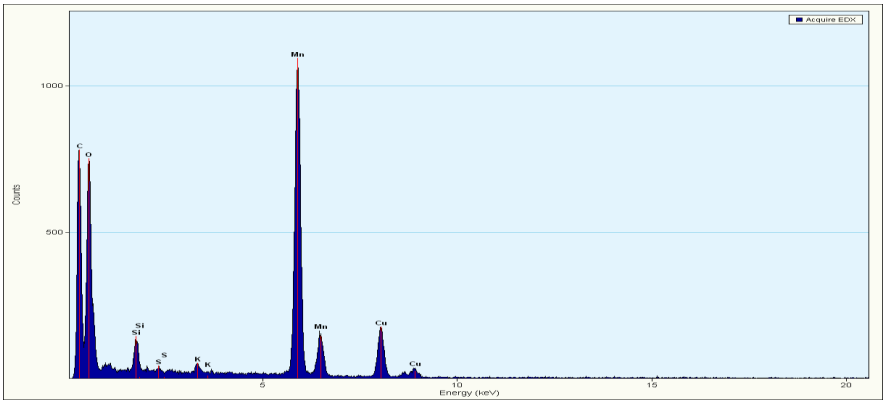

Fig 4. The EDS spectra of polyethylene glycol with Chloroquine

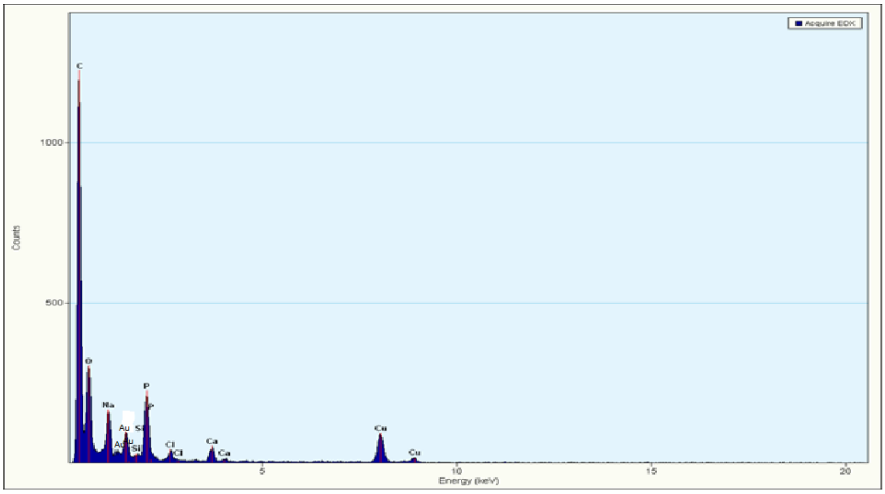

Fig 5. The EDS spectra of chemically synthesized gold nanoparticle sencapsulated with PEG and Chloroquine

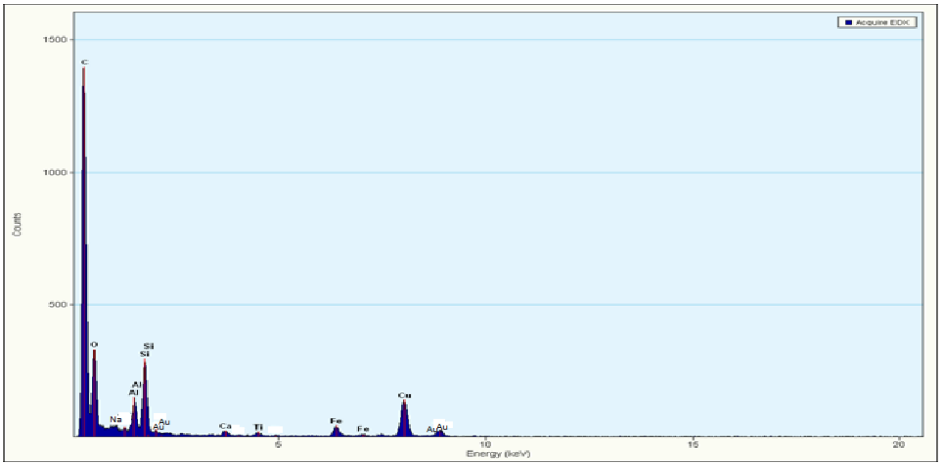

Fig 6. The EDS spectra of chemically synthesized gold nanoparticles encapsulated with PEG

low and very high concentrations of either reactant may lead to other by-products of the reaction.

Characterization of the encapsulations
Transmission electron microscopy

Transmission electron microscopy (TEM) images of the samples presented in Fig A-C show that the AuNPs are predominantly spherical with the small size distribution. The spherical morphology of the TEM images of the encapsulated AuNPs may be due to the sufficient volume of sodium citrate as a reducing agent and stirring. It causes an effective collision of the particle which prevents agglomeration of the AuNPs, thereby making monodispersed AuNPs. Furthermore, the TEM images show that the Chloroquine diphosphate is properly encapsulated into the spherical AuNPs for the purpose of target delivery. Khan et al. [25] reported that the spherical and nanotriangle shapes of AuNPs commonly used for drug delivery applications.

Energy-dispersive X-ray Spectroscopy of functionalized AuNPs

The EDS in Fig 4 shows that gold nanoparticle was not included in this formulation. However, signals were observed for different elements at different binding energies.

Carbon signal, oxygen, silicon, and potassium were approximately at 0.25, 0.50, 2.0, and 3.5 keV, respectively. Additional signals were obtained for manganese at 6.0, 6.5 and copper at 8.0 and 9.0 keV, respectively.

Figs 4 and 5 show the EDS of composites formulated with chemical synthesis of gold nanoparticles.

In Fig 4**,** the maximum absorption peak of gold located at 2.1 keV, whereas in Fig 5 it is located at 2, 2.1, and 9.9 keV. Both Figs show the presence of other additional signals for carbon-oxygen, silicon, phosphorus, calcium, and copper at 0.25, 0.5, 1.75, 2.5, 3.4, and 8.1 keV, respectively. However, signals for phosphorus and chlorine were observed in Fig 5 alone at approximate bonding energies of 2 and 2.6 keV.

Additional signals for calcium, titanium**,** and iron at 3.8, 4.5, and 7 keV are shown in Fig 6, respectively.

The presence of sodium may be attributed to sodium citrate as a reducing agent used for the synthesis. The iron, copper and carbon may come from holding the TEM grid.

Selected area electron diffraction patterns

The SAED of encapsulated gold nanoparticles are shown in Fig7 A-C which resulted in the characteristic ring pattern of face-centered cubic with multiple rings.

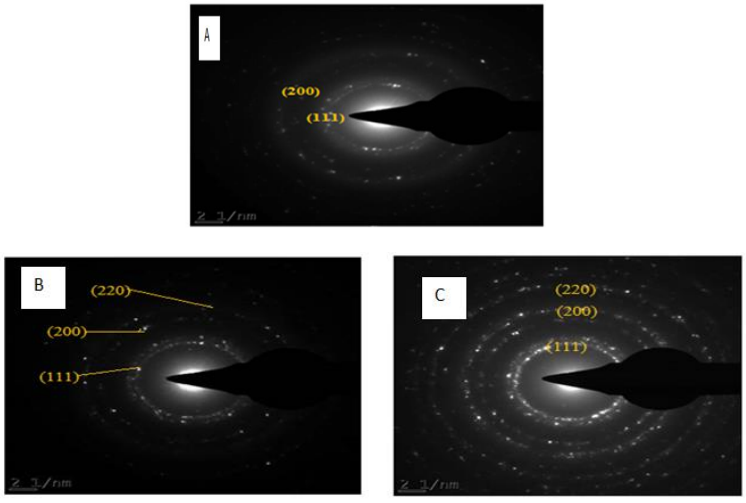

Fig 7. (A) The SAED pattern of PEG and Chloroquine (B) SAED pattern of chemically synthesized AuNPs functionalized with PEG and Chloroquine (C) SAED pattern of chemically synthesized AuNPs functionalized with PEG

Each ring represents diffraction from a specific crystal plane of similar sizes and different phases present in the gold nanoparticles.

Therefore, it shows the high degree of crystalline of AuNPs.

Moreover, the SAED pattern of the spherical gold nanoparticles revealed clear lattice fringes with bright circular rings corresponding to (111), (200), (220), and (311) planes.

In addition, there are several bright spots which are the effects of reflections from few individual crystals. In a study conducted by Malarkodi et al., strong intensities of AuNPs were shown at 111plane [26].

In vitro encapsulation release time

Fig 8 shows the concentration of encapsulation release time in phosphate buffer solution as a function of time.

It was observed that the Chloroquine phosphate entrapped with nanoparticle and PEG (PCND) has an extension time release, compared to the second formulation without the AuNPs (PD) whose release time terminated at 12 min.

Therefore, the slow release of the nano-entrapped formulated drug can be attributed to the high surface area and turnability of AuNPs which provides an excellent platform for the attachment of drug for controlled and sustained release.

According to the study conducted by Movellan et al. [20], the release of drug that had been trapped within the nanostructures during their preparation in water was attributed to drug solvent interactions and drug release that might be favored by the degradation of nanoparticles.

Moreover, embedding the drug in a complex matrix typically reduces its bioavailability, and in the case of immediate-release tablets, it has been reported to delay the onset of dissolution [12].

Antiplasmodial activity of encapsulation

Fig 9 presents the efficacy of reduction in the number of parasitized cell counts.

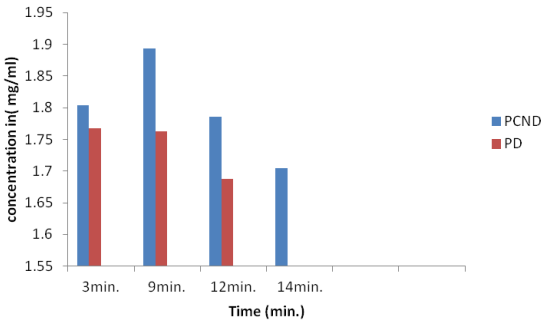

Fig 8. Release time-dependent on formulation for encapsulation
Key: PCND = PEG +CN-AuNPs +Chloroquine phosphate
PD = PEG + Chloroquine phosphate

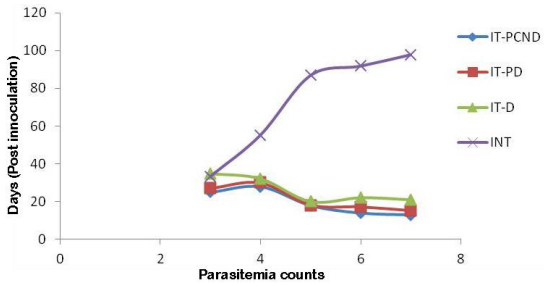

Fig 9. Effect of functionalized AuNPs on parasitaemia count in Plasmodium beighei infected mice

The total number of parasitized cell count shows a significant reduction in parasitemia count of the groups treated with the PCND (nano-entrapped), PD (without nano), and free Chloroquine diphosphate, compared to the infected untreated group. Despite the increase in a number of parasitized cell observed in the infected untreated group, the PCND, PD, and free Chloroquine diphosphate show antimalarial activity by reducing the cell count. Thereby, confirming the efficacy of the PCND, PD, and free Chloroquine diphosphate.

Histopathological studies

The photomicrograph of the liver of the mice treated with PCND, PD and free Chloroquine diphosphate is shown in plates VII and X. Tissues A and B showed necrosis, interphase hepatitis, ballooning degeneration, and bridging inflammation. However, tissues C showed generalized architectural disarray,

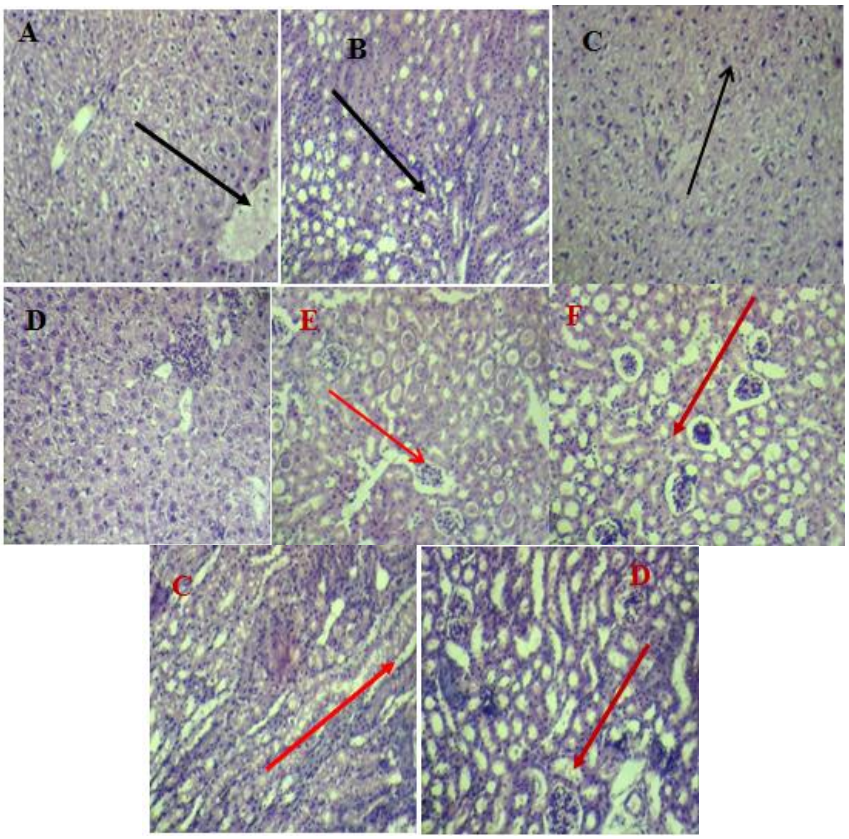

Fig 10. (A) Photomicrograph of mice liver after treatment with PCNCQ), (B) treatment with PD, (C) infected untreated group, (D) normal mice liver (control group) (E) Photomicrograph of mice kidney after treatment with PCNCQ, (F) treatment with PD (G) infected untreated group (H) normal mice liver (control group)

bridging, and periportal inflammation, acute necrosis, interphase, and periportal hepatitis and micro and macro vesicles.

Plates VII and X demonstrate normal tissues D with normal hepatocellular structures. Furthermore, plates XI and XIV show the photomicrographs of the kidney, which revealed tissues A and B with a tubular injury. However, tissues C show acute kidney damage, a subtle focal area, and the expansion of glomerulus, compared to normal tissues D showing normal histological structures.

The extent of damage in both liver and kidney (A) may be attributed to the chemicals used in the synthesis of the AuNPs that was used for the formulation of that composite [1]. With regard to tissues B, the inability of the standard drug to go straight to the target site and the first interaction with other cells resulted in unwanted side effects. Tissues D showed higher levels of damage because the animals are untreated and this resulted in the replication of more parasites destroying the red blood cells and consequently leading to the damage of the kidney.

However, the administration of nanoparticles may be either negative or positive effect since malarial parasites have the ability to cross the organs and cause liver damage which may eventually lead to kidney damage.

The entire treated group showed mild damage effects, compared to the untreated group.

CONCLUSION

The experimental results obtained revealed that the citrate reduction method

can be used to synthesiz AuNPs with a higher degree of monodispersity by controlling the ratio of gold salt to sodium citrate.

Moreover, high temperature and stirring rate lead to a decrease in AuNPs size. The nanoparticle-encapsulation shows antiplasmodial activity in vivo; however it is accompanied with some level of cytotoxicity on the liver and kidney of treated mice.

ACKNOWLEDGMENTS

This work was funded by the Tertiary Educational Trust Fund of Nigerian for TETFUND-Institutional based on research grant (TETFUND/FUTMINNA)/2015/31).

The authors express their gratitude to the Centre for Genetic Engineering and Biotechnology, Federal University of Technology, Minna, Nigeria, for its contribution to access to some of the nanotechnology facilities.

CONFLICT OF INTEREST

The authors declare that they have no conflict of interests.

REFERENCES

1.Crompton PD, Moebius J, Portugal S, Waisberg M, Hart G, Garver LS, Miller LH, Barillas-Mury C, Pierce SK. Malaria Immunity in man and Mosquito: Insights Into unsolved mysteries of a deadly infectious disease. Annu Rev Immunol. 2014; 32: 157-187.

2.Talisuna AO, Nalunkuma-Kazibwe A, Bakyaita N, Langi P, Mutabingwa TK, Watkins WW, Van Marck E, D'alessandro U, Egwang TG. Efficacy of sulphadoxine–pyrimethamine alone or combined with amodiaquine or chloroquine for the treatment of uncomplicated falciparum malaria in Ugandan children. Trop Med Int Health. 2004; 9(2): 222-229.

3.Nigussie D, Beyene T, Shah NA, Belew S. New Targets in Malaria Parasite Chemotherapy: A Review. Malaria Contr Elimination. 2015; S1:S1-007.

4.Singh R, Lillard JW Jr. Nanoparticle-based targeted drug delivery. Exp Mol Pathol. 2009; 86(3): 215–223.

5.Harish KK, Nagasamy V, Himangshu B, Anuttam K. Metallic Nanoparticle: A Review. Biomedical Journal of Scientific & Technical Research. 2018; 4(2)

6.Kumar A, BBM, Liang XJ. Gold nanoparticles: promising nanomaterials for the diagnosis of cancer and HIV/AIDS. J Nanomater. 2011; 2011: 1-17.

7.Almeida JPM, Chen AL, Foster A,Drezek R. In vivo biodistribution of nanoparticles. Nanomedicine(Lond). 2011; 6(5): 815-835.

8.Pooja D, Panyaram S, Kulhari H, Rachamalla SS, Sistla R. Xanthan gum stabilized gold nanoparticles: characterization, biocompatibility, stability and cytotoxicity. Carbohydr Polym. 2014; 110: 1-9.

9.Thakor AS, Jokerst J, Zavaleta C, Massoud TF, Gambhir SS. Gold nanoparticles: a revival in precious metal administration to patients. Nano Lett. 2011; 11(10): 4029–4036.

10.Kumar KP, Paul W, Sharma CP. Green synthesis of gold nanoparticles with Zingiber officinale extract: characterization and blood compatibility. Process Biochem. 2011; 46(10): 2007-2013.

11.Vilar G, Tulla-Puche J, Albericio F. Polymers and drug delivery systems. Curr Drug Deliv. 2012; 9(4): 367-394.

12.Markl D, Zeitler JA. A Review of Disintegration Mechanisms and Measurement Techniques. Pharm Res. 2017; 34(5): 890–917.

13.Kumari A, Yadav SK, Yadav SC. Biodegradable polymeric nanoparticles based drug delivery systems. Colloids Surf B Biointerfaces. 2010; 75(1): 1-18.

14.Li SD, Huang L. Stealth nanoparticles: high density but sheddable PEG is a key for tumor targeting. J Control Release. 2010; 145(3): 178.

15.Muller RH, Gohla S, Keck CM. State of the art of nanocrystals-special features production, nanotoxicology aspects and intracellular delivery. Eur J Pharm Biopharm. 2011; 78(1): 1-9.

16.Joshi P, Chakraborty S, Dey S, Shanker V, Ansari ZA, Singh SP. Binding of chloroquine-conjugated gold nanoparticles with bovine serum albumin. J Colloid Interface Sci. 2011; 355(2): 402-409.

17.Zhang X, Chibli H, Mielke R, Nadeau J. Ultrasmall gold-doxorubicin conjugates rapidly kill apoptosis-resistant cancer cells. Bioconjug Chem. 2011; 22(2): 235–243.

18.Movellan J, Urbán P, Moles E, Jesús M, Sierra T, Serrano JL, Fernandez-Busquets X. Amphiphilic dendritic derivatives as nanocarriers for the targeted delivery of antimalarial drugs. Biomaterials. 2014; 35(27): 7940-7950.

19.Urban P, Valle–Degado JJ, Mavro N, Marques J, Manfredi A, Rotman M, Ranucci E, Ferruti P, Fernàndez-Busquets X. Use of poly (amido amine) drug conjugates for the delivery of anti malarials to plasmodium. J Control Release. 2014; 177: 84-95.

20.Shittu KO, Bankole MT, Abdulkareem AS, Abubakar OK, Ubaka AU. Application of gold nanoparticles for improved drug efficiency. ADV NAT SCI-NANOSCI. 2017; 8(3): 14-35.

21.Kumar D, Meenan BJ, Dixon D. Glutathione-mediated release of Bodipy from PEG cofunctionalizationed gold nanoparticles. Int J Nanomedicine. 2012; 7: 4007.

22.Kumar D, Meenan BJ, Mutreja I, D'SA AR, Dixon D. Controlling the size and size distribution of gold nanoparticles: a design of experiment study. Int J

Nanosci. 2012; 11(2): 1250023.
23.Young JK, Lewinski NA, Langsner RJ, Kennedy LC, Satyanarayan A, Nammalvar V, Lin AY, Drezek RA. Drezek1Size-controlled synthesis of monodispersed gold nanoparticles via carbon monoxide gas reduction. Nanoscale Res Lett. 2011; (16)6: 428.
24.Haiss W, Thanh NT, Aveyard J, Fernig DG. Determination of Size and Concentration of Gold Nanoparticles from UV−Vis Spectra. Anal Chem. 2007; 79 (11): 4215–4221.
25.Khan AK, Rashid R, Murtaza G, Zahra A. Gold nanoparticles: synthesis and applications in drug delivery. TROP J PHARM RES. 2014; 13(7): 1169-1177.
26.Malarkodi C, Rajeshkumar S, Vanaja M, Paulkumar K, Gnanajobitha G, Annadurai G. Eco-friendly synthesis and characterization of gold nanoparticles using Klebsiella pneumoniae. J Nanostructure Chem. 2013; 3(1): 30.